Some mathematical questions arising from demography: How long we can live in the USA?

Oscar Angulo*, Juan Carlos López-Marcos*
and Fabio Augusto Milner†

Abstract

Many age-structured demographic models assume that the mortality rate is bounded, leading to immortality for some individuals. Other models assume a maximal finite age for the population, leading to unbounded mortality rates. In a realistic age-structured model no individual can live indefinitely and, in consequence, mortality must tend to infinity as age approaches the maximal one. However, such maximal age is not determined from physical or biological principles but rather depends on the particular population under consideration. We consider here the problem of identifying the maximal possible age for the present female population of the USA, and we propose a practical numerical method to accurately approximate the age density of that population all the way to the maximal age. We exemplify the limitations the data impose on the quality of the projections of this model through a 10-year simulation for the USA from 1990 to 2000. Finally, we project the population of the USA in 2010 using this model.

1 Introduction

Demographic models have evolved from simple, unstructured ones to fairly sophisticated structured ones that subdivide the population under study according to characteristics such as age, sex, race, and others. The most widely used structure variable is age, since it is important to know, for example, the number of school-age children or individuals past retirement age for educational and social security planning respectively.

As we shall see later on in this paper, projecting the size of cohorts of advanced age is a difficult problem. Yet this is a very important issue for planning purposes since fairly accurate estimates of the size of those cohorts are needed in order to forecast and plan the funding of medical care, retirement facilities, and geriatric services, for example.

For many other purposes, though, the cohorts of advanced age are inconsequential and may be ignored altogether. Examples of important demographic issues unaffected by older age cohorts include the number of children of school age or women of reproductive age. In order to

*Departamento de Matemática Aplicada, Universidad de Valladolid, 47014 Valladolid, Spain
†Department of Mathematics, Purdue University, 150 North University St., West Lafayette, IN 47907-2067

make projections about the sizes of cohorts such as these one can assume that the mortality is bounded and not worry about projecting past a certain age.

One of the problems associated with age structure at advanced ages is that of the maximal age of a population. For biological reasons it is clear that every individual must die in finite time or, better said, may not reach an arbitrarily large age. The problem resulting from the existence of a maximal age is twofold: first, such age is not predetermined from biological or physical laws but must rather be determined from the population data; secondly, from a mathematical standpoint, its existence precludes the desirable and frequently made assumption that the mortality rate is bounded. The fact that every individual must die before reaching that age requires the mortality to become infinite as the age approaches the maximal one that we shall denote as $a_\dagger$. In fact, it is easy to see that not only must the mortality rate approach infinity, but also its integral on the age interval $[0, a_\dagger)$ must be infinite.

Iannelli and Milner [4] showed one way to modify general finite difference methods in order to accommodate unbounded mortality and still preserve globally the local order of convergence. It was shown in that work that the mortality rate needs to approach infinity sufficiently fast as the age approaches the maximal one. They also showed that this requirement is fulfilled by functions of the form $\mu(a) = \frac{C}{(a_\dagger - a)^\alpha}$ with $\alpha \geq 1$ for a in the interval $[A^*, a_\dagger)$.

In this paper we shall first attempt to determine from such form of the mortality rate the maximal age for the female population of the United States of America, using least squares fitting of mortality data obtained from life tables for the years 1990 and 2000. Once a credible value for the maximal age is established, we shall use it to run a 10-year simulation of that population using census data for the years 1990 and 2000, and mortality and fertility rates available from vital statistics tables of the USA. We shall use vital rates that are constant-in-time, as well as linear interpolations of those for the years 1990 and 2000. The purpose of these simulations is to bring to light some important limitations inherently present in projecting population densities due to immigration and inconsistency in the available vital rates, as well as the role of the choice of fitting for the latter in order to define the vital rate functions needed for simulations. Immigration accounts for significant changes in population size for some age cohorts but it is very difficult to model since it is largely dependent upon government policy and prevailing economic conditions abroad. The demographic model we use ignores immigration and is based just on the birth and death process.

Finally, in order to make projections for the future, we shall fit mortality and fertility data for the period from 1970 to 2000 for each age cohort, in order to establish trends by age. We shall then define extrapolated mortality and fertility rates based on those trends for the time variable, using linear interpolation among the cohorts in the age variable. Using the vital rates thus defined together with census data for the year 2000, we shall make a projection of the population for the year 2010.

The present paper is organized as follows: in the next section we present the demographic model due to McKendrick and von Foerster and recall some analytic properties it has. In Section 3 we describe in detail the available data and how it is used to produce the functions the model needs, and in Section 4 we describe the numerical method we shall employ and prove that it converges at second order. In Section 5 we present the results from our numerical experiments, and in Section 6 we make some concluding remarks.

2 Formulation of the Problem

We consider the problem of modeling the evolution of the age density of the female population of the United States as described by the McKendrick von Foerster model,

$$\begin{cases} u_t + u_a = -\mu(a,t)\, u, & a \in (0, a_\dagger),\ t \in (0,T), \\ u(0,t) = \displaystyle\int_0^{a_\dagger} \beta(a,t)\, u(a,t)\, da, & t \in (0,T), \\ u(a,0) = u_0(a), & a \in [0, a_\dagger), \end{cases} \tag{1}$$

where $u(\cdot, t)$ is the age density of the population at time t, $\mu(\cdot)$ is the age specific mortality rate, $\beta(\cdot)$ is the age specific fertility rate, and $u_0(\cdot)$ is the initial age density.

When the system is autonomous, i.e. mortality and fertility rates do not depend on time, there is a simple condition for the existence of steady steady states, namely that the *intrinsic reproductive number* of the population be equal to unity:

$$\mathcal{R}_0 = \int_0^{a_\dagger} \beta(a)\, \Pi(a)\, da = 1,$$

where

$$\Pi(a) = \exp\left(-\int_0^a \mu(s)\, ds\right)$$

is the survival function representing the probability at birth of surviving to a age a. Since $a_\dagger$ is the maximal age, it is necessary that $\Pi(a_\dagger) = 0$. It then follows that

$$\int_0^{a_\dagger} \mu(s)\, ds = +\infty,$$

and, *a fortiori*, $\lim_{a \to a_\dagger} \mu(a) = +\infty$. It can be shown that the steady states are multiples of the survival probability and that they represent the ultimate age profile of the population in the sense that, for any $\mathcal{R}_0 > 0$, there is a function $\Omega(\cdot)$ such that $\lim_{s\to\infty} \Omega(s) = 0$, and

$$u(a,t) = e^{\lambda^*(t-a)}\, \Pi(a)\, [b_0 + \Omega(t-a)]\,,$$

where λ^* is the *Malthusian growth rate* of the population, that is, the only real root of the characteristic equation

$$\int_0^{a_\dagger} e^{-\lambda s} \beta(s)\, \Pi(s)\, ds = 1.$$

It is easy to see that $\mathcal{R}_0 > 1 \Leftrightarrow \lambda^* > 0$, $\mathcal{R}_0 = 1 \Leftrightarrow \lambda^* = 0$, and $\mathcal{R}_0 < 1 \Leftrightarrow \lambda^* < 0$,

Integration along the characteristics leads to the following semi-explicit expression for the age density:

$$u(a,t) = \begin{cases} u_0(a-t)\, \dfrac{\Pi(a)}{\Pi(a-t)}, & a \geq t, \\ B(t-a)\, \Pi(a), & a < t, \end{cases}$$

where $B(\cdot) = u(0, \cdot)$ is the total fertility rate. This function is the unique solution of the *renewal equation*

$$B(t) = F(t) + \int_0^\infty K(t - s)B(s)\, ds,$$

where $K = \beta\,\Pi$ is the net maternity function, and

$$F(t) = \int_0^\infty \beta(a + t)\frac{\Pi(a + t)}{\Pi(a)}\, u_0(a)\, da.$$

In the non-autonomous case B is still the solution of a Volterra integral equation, but not in convolution form. The renewal equation is the basis for the derivation of many analytical results, as well as for some numerical methods.

3 Data functions

We select the regularity for the data functions based on the order of convergence of the numerical method, and we build them from the data available from tables of vital statistics and census information. Gathering the information the model needs is not a trivial task. Some data is found in one format (e.g. fertility is reported in 5-year age cohorts) while other data in a different format (e.g. census data or life tables may be available in 1-year cohorts). To make matters even worse, data is not consistent. For example, the birth rates obtained as ratios of the number of offspring borned by women in a given age cohort to that cohort size does not match the rates reported in vital statistics tables such as the one we show below. Therefore, we decided to define the age specific birth and death rates, and the initial age distribution of the population, from the data we expect will lead to the smallest errors.

For the birth rate, we use the rates reported in vital statistics tables in 5- year cohorts (with two exceptions: the 15-to-17-year-olds and the 18-to-19-year-olds). We define the birth rate either by linear interpolation into a continuous function or directly by the data as a piecewise constant function of age.

For the mortality rates we use a life table from which we derive the mortality rate as explained below, since we obtain this way data in 1-year cohorts that leads to a more accurate mortality than 5-year cohorts.

We do our simulations for the decade from 1990 to 2000 using both constant-in-time vital rates and linear-in-time interpolations of the mortality functions we define for 1990 and for 2000 and piecewise linear-in-time interpolations of the fertility functions we define for each year from 1990 to 2000. For the projections for the year 2010, we do simulations using both a constant-in-time vital rates or age-cohort-by-cohort extrapolations of historical mortality data from 1970 to 2000.

For the year 1990 we have the age distribution in age cohorts of variable size (between 1 and 5 years) and for 2000 we have them year by year. Therefore, since the life tables for both years give the year-by-year data until age 100, we use the life table as the basis for the derivation of the mortality rates.

3.1 Mortality, $\mu(a)$.

We impose the following four requirements to the age-specific mortality:

- Continuous for $a \in [0, a_\dagger)$, where the maximal age $a_\dagger$ needs to be determined.
- Piecewise linear up to $A^* = 80$.
- Quadratic polynomial from A^* to $A_* = 100$, with continuity at A^*. We make this choice because the data can be fitted extremely well by a quadratic polynomial.
- Of the form $\mu(a) = \frac{C}{(a_\dagger - a)^\alpha}$ from A_* to $a_\dagger$, where $a_\dagger$ is determined first, from mortality data using a least squares fit of the available mortality data for the three constants C, $a_\dagger$, and α. The value of $a_\dagger$ thus found is then used to determine C and α such that the data to the left and to the right of A_* fit continuously, with continuous first derivative.

The quadratic polynomial is the first piece we define, using a least squares fit of the mortality data for ages from A^* to A_*. We use the twenty values of the year-by-year mortality rates derived for those ages from the life tables found in United States Vital Statistics [6] as the values of the function μ at the points $a = j + \frac{1}{2}$ for $80 \leq j \leq 99$. Then we use the values of this least squares quadratic polynomial to determine the values of C and α for μ as explained above.

After we have defined the function for $a \in [A^*, a_\dagger)$, we proceed from right to left, year by year, defining $\mu(n + \frac{1}{2}) = \mu_n$, where μ_n is the value of the mortality rate derived from life tables for $a \in [n, n+1)$.

We start from the value $\mu(A^*)$ defined by this quadratic polynomial. The values of the probability of survival, $\Pi(a)$, are the main piece of information found in the life table. Since they are analytically given by

$$\Pi(a) = \exp\Big(-\int_0^a \mu(s)\, ds\Big),$$

we see that

$$\int_j^{j+1} \mu(s)\, ds = \ln\left(\frac{\Pi(j)}{\Pi(j+1)}\right),$$

and this relation leads to the following midpoint approximation:

$$\mu_j = \mu\Big(j + \frac{1}{2}\Big) \approx \ln\left(\frac{\Pi(j+1)}{\Pi(j)}\right). \qquad (2)$$

Next, on the interval $[79.5, 80]$ we define the graph of the mortality rate as the segment joining the points $(79.5, \mu(79.5))$ and $(80, \mu(80))$. On any given age interval $[j + \frac{1}{2}, j + \frac{3}{2}]$ $(0 \leq j \leq 78)$, using the values μ_j and μ_{j+1}, we define the graph of the mortality rate as the segment joining the points $(j + \frac{1}{2}, \mu(j + \frac{1}{2}))$ and $(j + \frac{3}{2}, \mu(j + \frac{3}{2}))$. In the interval $[0, \frac{1}{2}]$ the mortality is defined by extending the segment joining $(0.5, \mu(0.5))$ and $(1.5, \mu(1.5))$.

We show below the graph of the survival function Π taken from the life table [7].

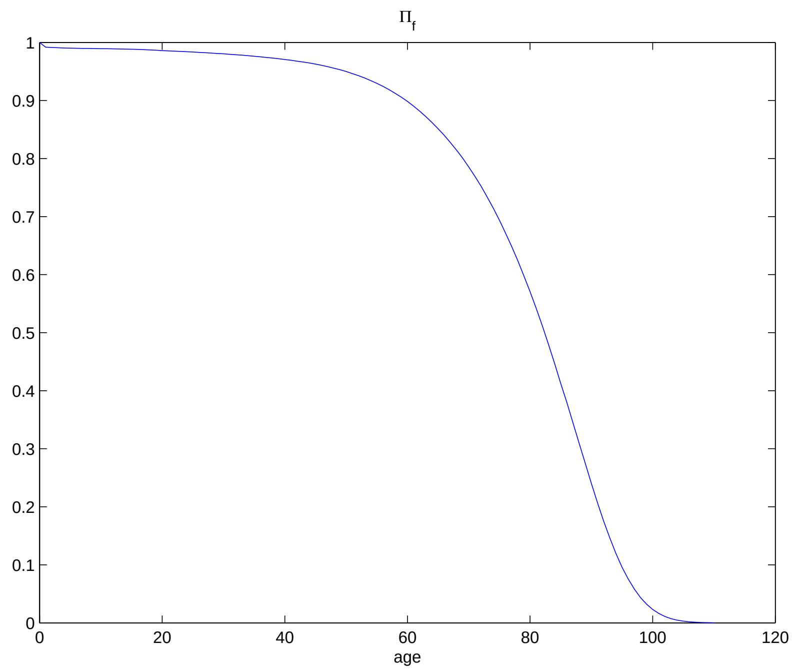

Figure 1: Probability of survival for females, United States, 2000

The graph of the resulting mortality rate is shown below:

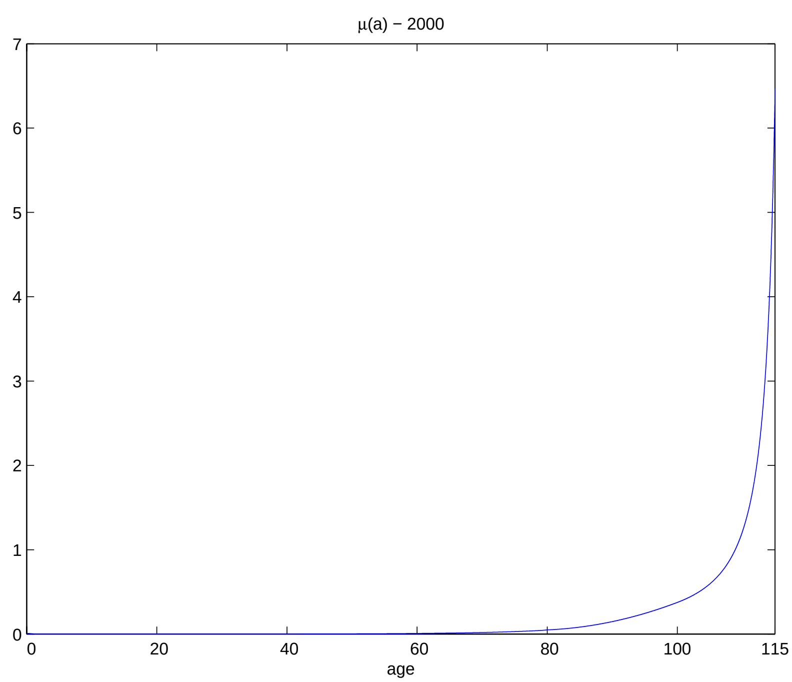

Figure 2: Mortality rate derived from survival data, United States, 2000

The next figure shows the graph of the mortality rate where it is defined as a piecewise linear function, that is for $0 \leq a \leq 80$, for 1990 in red and for 2000 in blue.

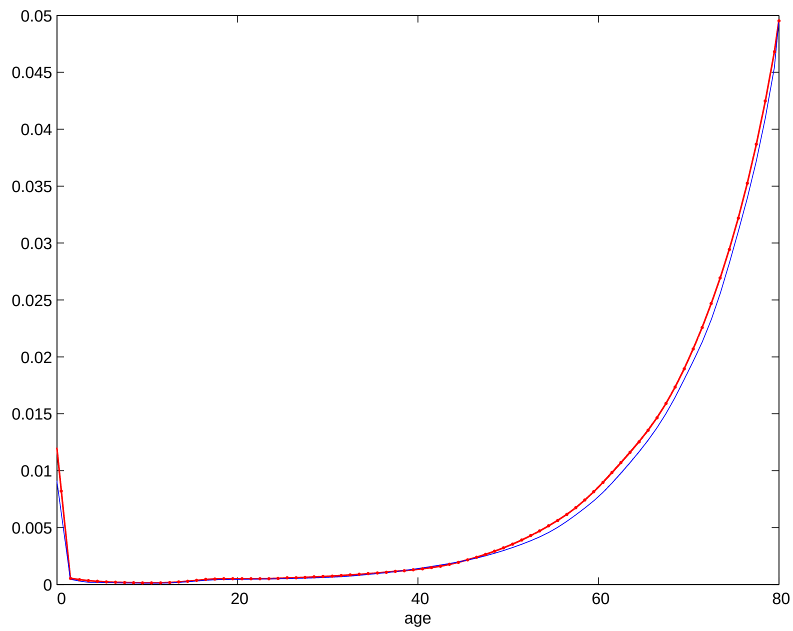

Figure 3: Change in mortality rate, United States, 1990 to 2000

Note that the derivative is allowed to be discontinuous at $a = n + \frac{1}{2}$, $1 \leq n \leq A^*$, as is apparent at $a = 1.5$. During the decade from 1990 to 2000 female mortality in the U.S. decreased for most age cohorts, as seen in Figure 3.

3.2 Fertility, $\beta(a)$

We use several forms for the fertility function, some independent of time, some dependent on both age and time. For time-dependent fertility we shall use for each year from 1990 to 2000 a piecewise linear or piecewise constant in age function defined exactly as indicated below for 1990 in the time-independent case. The time dependence will then be included either as piecewise constant or piecewise linear over each year from 1990 to 2000.

For the time-independent fertility, we shall define two different functions, one piecewise linear in age, the other piecewise constant. We build the piecewise linear fertility rate subject to the following constraints:

- Continuous for $a \in [0, a_\dagger)$.
- Piecewise linear in age, constant in time.
- Compactly supported in the *fertility window* $[10, 50]$.

First we extract the values given in the vital statistics for the year 1990 for the various age cohorts, 10-14, 15-17, 18-19, 20-24, 25-29, 30-34, 35-39, 40-45, and 45-49. Each of these values is assigned to the mean age of the corresponding cohort, e.g. $\beta_{16.5} = 0.0375$ is the value reported for the cohort of women aged 15 to 17. We define $\beta_{10} = \beta_{50} = 0$. For each pair of midpoints of two consecutive age cohorts, $\bar{a}_j$ and $\bar{a}_{j+1}$, we then define the graph of β by joining the points

$(\bar{a}_j, \beta_{a_j})$ and $(\bar{a}_{j+1}, \beta_{a_{j+1}})$. The first and last nontrivial linear pieces are defined, respectively, by joining the points $(10, 0)$ with $(12.5, \beta_{12.5})$ and $(47.5, \beta_{47.5})$ with $(50, 0)$.

The data is drawn from the Vital Statistics of the United States [7]. We show below the table from which we take all the fertility data for this paper.

Table 1. Number of births, crude birth rates, general fertility rates, total fertility rates, and birth rates, by age and race of mother: United States, 1990–2001

[Birth rates are live births per 1,000 population in specified group. Fertility rates are live births per 1,000 women aged 15–44 years in specified group. Total fertility rates are sums of birth rates for 5-year age groups multiplied by 5. Age-specific rates are live births per 1,000 women in specified age and racial group. Population enumerated as of April 1 for 1990 and 2000 and estimated as of July 1 for all other years. Rates for 1991–2001 have been revised using population estimates based on the 2000 census, and may differ from rates previously published; see text and "Technical Notes"]

Year and race	Number of births	Crude birth rate	General fertility rate	Total fertility rate	Age of mother									
					10–14 years	15–19 years			20–24 years	25–29 years	30–34 years	35–39 years	40–44 years	45–49 years[1]
						Total	15–17 years	18–19 years						
All races[2]														
2001	4,025,933	14.1	65.3	2,034.0	0.8	45.3	24.7	76.1	106.2	113.4	91.9	40.6	8.1	0.5
2000	4,058,814	14.4	65.9	2,056.0	0.9	47.7	26.9	78.1	109.7	113.5	91.2	39.7	8.0	0.5
1999	3,959,417	14.2	64.4	2,007.5	0.9	48.8	28.2	79.1	107.9	111.2	87.1	37.8	7.4	0.4
1998	3,941,553	14.3	64.3	1,999.0	1.0	50.3	29.9	80.9	108.4	110.2	85.2	36.9	7.4	0.4
1997	3,880,894	14.2	63.6	1,971.0	1.1	51.3	31.4	82.1	107.3	108.3	83.0	35.7	7.1	0.4
1996	3,891,494	14.4	64.1	1,976.0	1.2	53.5	33.3	84.7	107.8	108.6	82.1	34.9	6.8	0.3
1995	3,899,589	14.6	64.6	1,978.0	1.3	56.0	35.5	87.7	107.5	108.8	81.1	34.0	6.6	0.3
1994	3,952,767	15.0	65.9	2,001.5	1.4	58.2	37.2	90.2	109.2	111.0	80.4	33.4	6.4	0.3
1993	4,000,240	15.4	67.0	2,019.5	1.4	59.0	37.5	91.1	111.3	113.2	79.9	32.7	6.1	0.3
1992	4,065,014	15.8	68.4	2,046.0	1.4	60.3	37.6	93.6	113.7	115.7	79.6	32.3	5.9	0.3
1991	4,110,907	16.2	69.3	2,062.5	1.4	61.8	38.6	94.0	115.3	117.2	79.2	31.9	5.5	0.2
1990	4,158,212	16.7	70.9	2,081.0	1.4	59.9	37.5	88.6	116.5	120.2	80.8	31.7	5.5	0.2

We now include a bar graph with the mid-cohort values we use to define this piecewise-linear fertility rate β.

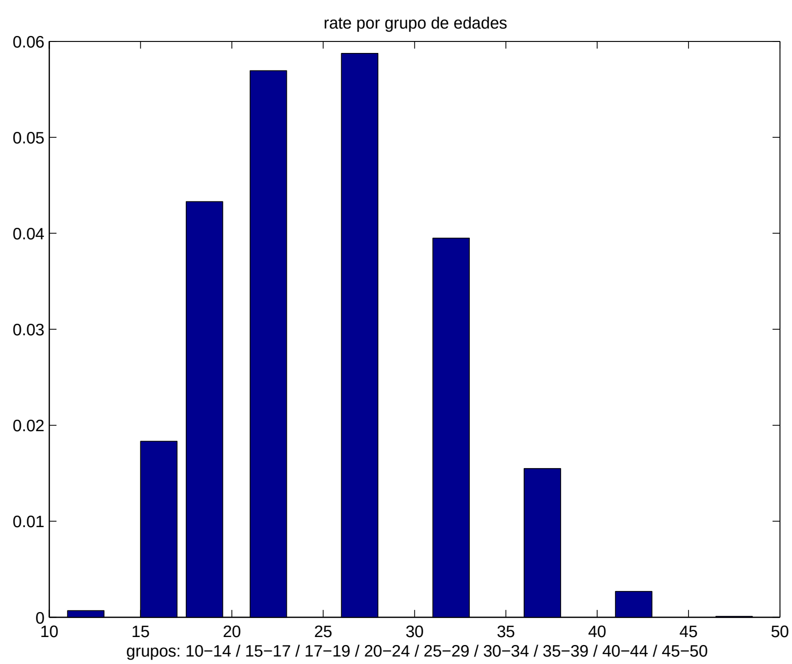

Figure 4: Histogram of fertility data, United States, 1990

Below we show the graph of the resulting piecewise linear fertility function.

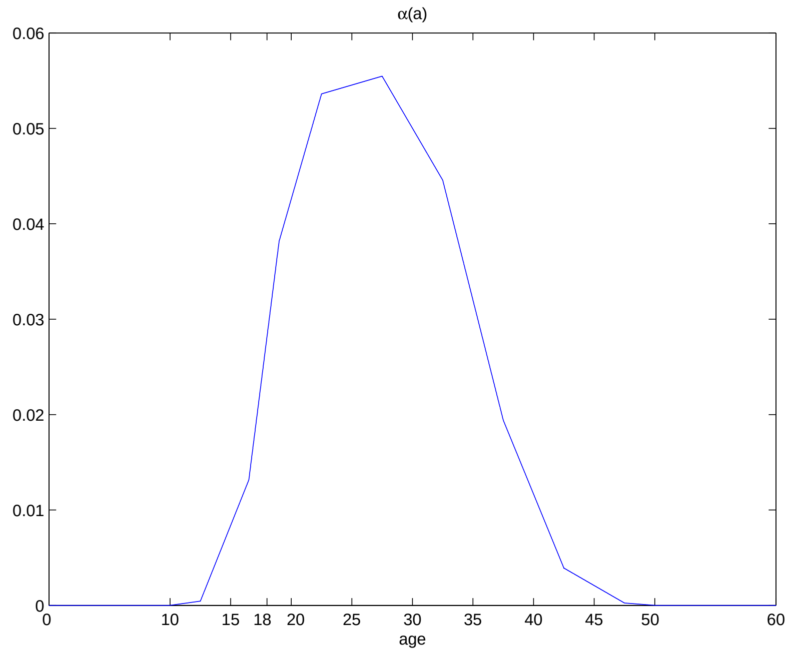

Figure 5: Piecewise linear fertility rate, United States, 1990

Note that, just as with the mortality rate, we allow the discontinuity of the derivative of the fertility rate at the points where consecutive linear segments meet.

Finally, we show the graph of the piecewice constant fertility rate defined by the bar graph in Figure 4 which we shall use in our simulations.

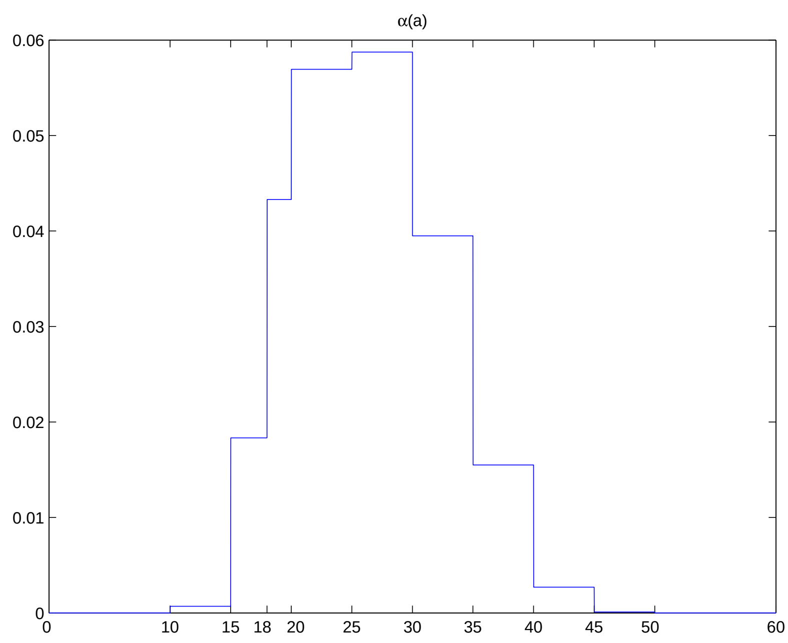

Figure 6: Piecewise constant fertility rate, United States, 1990

3.3 Initial Condition, $u_0(a)$

For initial data we use the age distribution reported by the National Bureau of Census and Statistics for the year 1990. We choose three different options for defining u_0, depending on the regularity desired for the utilization of particular numerical methods. Reduced regularity may result in some numerical methods converging at a suboptimal rate.

- First Option: Global regularization and compatibility at $a = t = 0$. We impose the following conditions:

  - Quadratic splines for each age cohort.
  - Globally continuous with continuous derivative.
  - $u_0(a_\dagger) = 0$
  - Compatibility at $a = t = 0$, that is $u_0(0) = \int_0^{a_\dagger} \beta(a)\, u_0(a)\, da$.

  The graph of the resulting initial distribution is

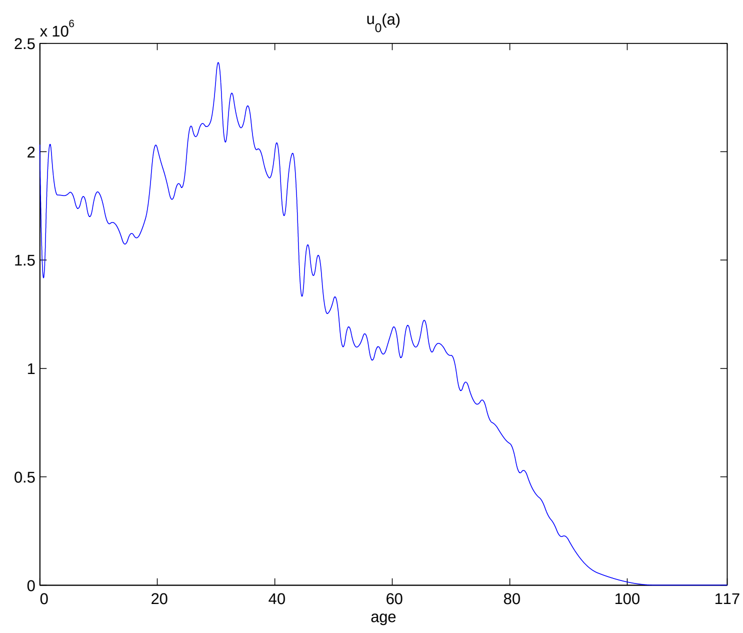

Figure 7: Regularized female age density, United States, 1990

- Second Option: Global regularization without compatibility at the origin. We impose the following conditions:

  - Globally continuous.
  - Piecewise linear.
  - $u_0(a_\dagger) = 0$

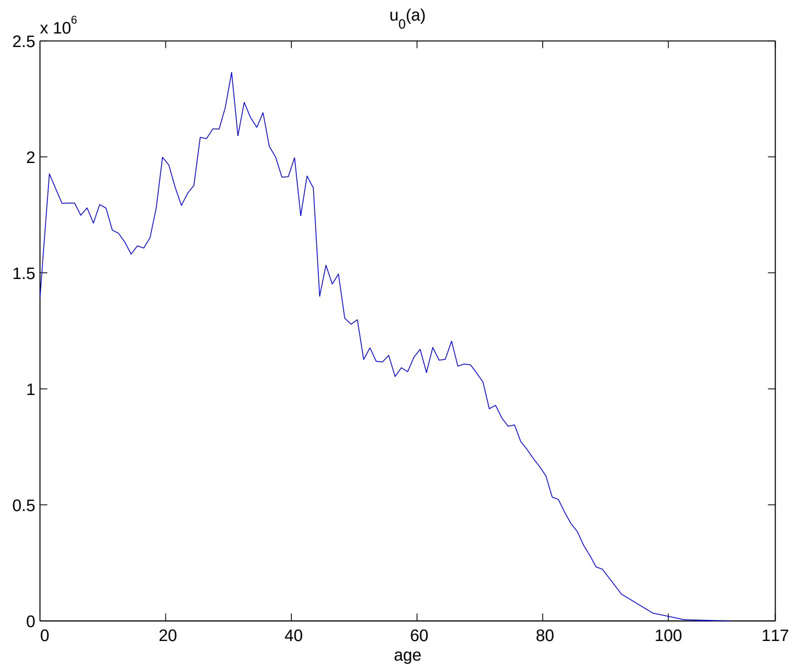

Figure 8: Regularized female age density without compability, United States, 1990

- Third Option: Utilize the data from the table directly. This imposes the following properties:
  - Discontinuous piecewise constant.

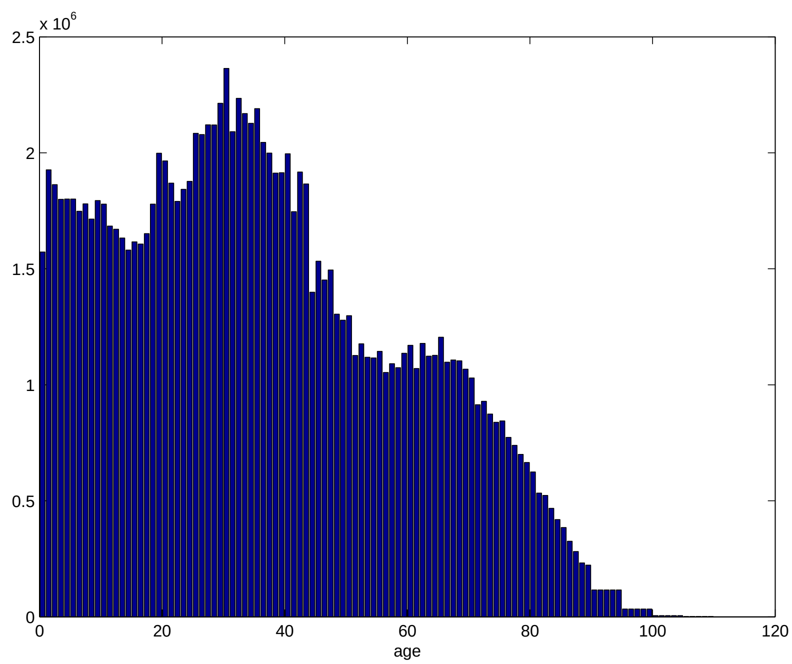

Figure 9: Piecewise constant female age density, United States, 1990

4 Numerical method

We start from the analytic representation of the solution:

$$u(a+k,t+k) = u(a,t)\,\exp\left(-\int_0^k \mu(a+\tau,t+\tau)\,d\tau\right), \tag{3}$$

where $0 \le k \le a_\dagger - a$. We now choose a final time for the numerical solution, T, and the number of steps we want to use to arrive at this final time, N. Then we define the discretization parameter $k = \frac{T}{N}$, and let $J = \left[\frac{a_\dagger}{k}\right]$ be the number of steps needed to cover the age interval $[0, a_\dagger)$. Without loss of generality we assume J is an integer greater than 1.

We shall use the following notation: $J^* = \left[\frac{A^*}{k}\right] + 1$, $a_j = j\,k$, for $0 \le j \le J$, $t^n = n\,k$ for $0 \le n \le N$; U_j^n will be the numerical approximation of $u(a_j, t^n)$ that we now proceed to define.

$$\left\{\begin{array}{lll} U_j^0 & = & u_0(a_j), \qquad 0 \le j \le J, \\ U_{j+1}^{n+1} & = & U_j^n\,\exp\left(-k\,\mu\left(a_j + \frac{k}{2}, t^n + \frac{k}{2}\right)\right), \qquad 0 \le j \le J^* - 1,\ 1 \le n \le N-1, \\ U_{j+1}^{n+1} & = & U_j^n\,\exp\left(-\int_0^k \mu(a_j + s, t^n + s)\,ds\right), \qquad J^* \le j \le J-1,\ 1 \le n \le N-1, \\ U_0^{n+1} & = & \dfrac{k}{2}\displaystyle\sum_{j=1}^{J}\left[\beta(a_{j-1}, t^{n+1})\,U_{j-1}^{n+1} + \beta(a_j, t^{n+1})\,U_j^{n+1}\right], \qquad 0 \le n \le N-1. \end{array}\right. \tag{4}$$

We shall show that the convergence of the numerical approximation thus defined to the analytic solution of the non-autonomous McKendrick-von Foerster model is of second order.

Let us introduce the following notation for the pointwise error:

$$\varepsilon_j^n = u(a_j, t^n) - U_j^n, \tag{5}$$

and the following discrete norms:

$$\|\varepsilon\|_{l^\infty(l^\infty)} = \max_{\substack{0 \le j \le J \\ 0 \le n \le N}} \{|\varepsilon_j^n|\}, \quad \|\varepsilon^n\|_{l^1} = \sum_{j=0}^{J-1} k|\varepsilon_j^n|, \quad \|\varepsilon\|_{l^\infty(l^1)} = \max_{0 \le n \le N} \{\|\varepsilon^n\|_{l^1}\} \tag{6}$$

Theorem 4.1: Assume that the solution of the McKendrick-von Foerster model (1) is sufficiently regular. Then, there exists a constant $Q > 0$, independent of k, such that

$$\|\varepsilon\|_{l^\infty(l^1)} \le Qk^2 \qquad \text{and} \qquad \|\varepsilon\|_{l^\infty(l^\infty)} \le Qk^2. \tag{7}$$

Proof. Note that (3) gives, for $0 \le j \le J-1$ and $0 \le n \le N-1$, the relation

$$u(a_{j+1}, t^{n+1}) = u(a_j, t^n)\,\exp\left(-\int_0^k \mu(a_j + s, t^n + s)\,ds\right). \tag{8}$$

We now subtract (4.ii) from (8) side by side and using (5), we obtain the relation

$$\begin{aligned}\varepsilon_{j+1}^{n+1} &= u(a_j,t^n)\left[\exp\left(-\int_0^k \mu(a_j+s,t^n+s)\,ds\right)-\exp\Bigl(-k\,\mu(a_j+\tfrac{k}{2},t^n+\tfrac{k}{2})\Bigr)\right]\\ &\quad+\exp\Bigl(-k\,\mu(a_j+\tfrac{k}{2},t^n+\tfrac{k}{2})\Bigr)\,\varepsilon_j^n, \qquad 0\le j\le J^*-1,\ 0\le n\le N-1.\end{aligned} \tag{9}$$

Let now $K_1 = \|u\|_{L^\infty\left([0,a_\dagger)\times[0,T]\right)}$ and $K_2 = \|D^2\mu\|_{L^\infty\left([0,A^*]\times[0,T]\right)}$. Taking absolute value on both sides of (9) and using the mean value theorem and the standard error bound for the midpoint quadrature rule, we are led to

$$\left|\varepsilon_{j+1}^{n+1}\right| \le \left|\varepsilon_j^n\right| + \frac{K_1K_2}{24}\,k^3, \qquad 0\le j\le J^*-1,\ 0\le n\le N-1. \tag{10}$$

Similarly, subtracting (4.iii) from (8) side by side and using (5), we are led to

$$\varepsilon_{j+1}^{n+1} = \varepsilon_j^n\,\exp\left(-\int_0^k \mu(a_j+s,t^n+s)\,ds\right), \qquad J^*\le j\le J-1,\ 0\le n\le N-1,$$

whereby

$$|\varepsilon_{j+1}^{n+1}| \le |\varepsilon_j^n|, \qquad J^*\le j\le J-1,\ 0\le n\le N-1. \tag{11}$$

Note that, even though unnecessary for this bound, the integral in (4.iii) can be evaluated exactly, since μ is either a quadratic polynomial or the reciprocal of a power function on the interval of integration. For example, for $j\ge J_*$ in (4.iii), $\mu(a) = \dfrac{C}{(a_\dagger - a)^\alpha}$ gives

$$\Pi(a) = \exp\left(-\frac{C}{\alpha-1}\left[\frac{1}{(a_\dagger-a_{j+1})^{\alpha-1}} - \frac{1}{(a_\dagger-a_j)^{\alpha-1}}\right]\right).$$

Next, we recall the following error bound for the composite trapezoidal quadrature rule:

$$\begin{aligned}&\left|\int_0^{a_\dagger}(\beta\,u)(a,t^{n+1})\,da - \frac{k}{2}\sum_{j=1}^{J}\Bigl[(\beta\,u)(a_{j-1},t^{n+1}) + (\beta\,u)(a_j,t^{n+1})\Bigr]\right|\\ &\qquad\qquad \le K_3\,\|D^2(\beta u)\|_{L^\infty\left([0,A^*]\times[0,T]\right)}\,k^2,\end{aligned} \tag{12}$$

where the constant K_3 is independent of k. We combine now (1.ii) with (4.iv) and (12) to see that

$$\begin{aligned}|\varepsilon_0^{n+1}| &\le \left|\int_0^{a_\dagger}(\beta\,u)(a,t^{n+1})\,da - \frac{k}{2}\sum_{j=1}^{J}\Bigl[(\beta\,u)(a_{j-1},t^{n+1}) + (\beta\,u)(a_j,t^{n+1})\Bigr]\right|\\ &\quad+\frac{k}{2}\sum_{j=1}^{J}\Bigl[\beta(a_{j-1},t^{n+1})\,|\varepsilon_{j-1}^{n+1}| + \beta(a_j,t^{n+1})\,|\varepsilon_j^{n+1}|\Bigr]\\ &\le K_3\,\|D^2(\beta u)\|_{L^\infty\left([0,A^*]\times[0,T]\right)}\,k^2 + \|\beta\|_{L^\infty\left([0,a_\dagger)\times[0,T]\right)}\,\|\varepsilon^{n+1}\|_{l^1}.\end{aligned} \tag{13}$$

Multiplying (10), (11), and (13) by k and summing the resulting relations side-by-side for $0 \le j \le J-1$, we see that

$$\|\varepsilon^{n+1}\|_{l^1} \le \|\beta\|_{L^\infty\left([0,a_\dagger)\times[0,T]\right)} k\,\|\varepsilon^{n+1}\|_{l^1} + \|\varepsilon^n\|_{l^1} + K_4\,k^3, \tag{14}$$

where $K_4 = K_3\,\|D^2(\beta u)\|_{L^\infty\left([0,A^*]\times[0,T]\right)} + \dfrac{K_1K_2}{24}\,,(A^*+1)$. If we now assume that $k < \dfrac{1}{2\|\beta\|_{L^\infty\left([0,a_\dagger)\times[0,T]\right)}}$ then (14) implies that

$$\|\varepsilon^{n+1}\|_{l^1} \le \left(1 + 2\|\beta\|_{L^\infty\left([0,a_\dagger)\times[0,T]\right)} k\right)\left(\|\varepsilon^n\|_{l^1} + K_4\,k^3\right),$$

which, iterated into itself, leads to the relation

$$\begin{aligned}\|\varepsilon^{n+1}\|_{l^1} &\le \left(1 + 2\|\beta\|_{L^\infty\left([0,a_\dagger)\times[0,T]\right)} k\right)^{n+1}\|\varepsilon^0\|_{l^1} + K_4\,k^3\sum_{m=1}^{n+1}\left(1 + 2\|\beta\|_{L^\infty\left([0,a_\dagger)\times[0,T]\right)} k\right)^m \\ &\le e^{2\,T\,\|\beta\|_{L^\infty\left([0,a_\dagger)\times[0,T]\right)}}\,\|\varepsilon^0\|_{l^1} + \frac{e^{2\,(T+1)\,\|\beta\|_{L^\infty\left([0,a_\dagger)\times[0,T]\right)}}}{2\|\beta\|_{L^\infty\left([0,a_\dagger)\times[0,T]\right)}} K_4\,k^2.\end{aligned} \tag{15}$$

Next we note that (1.iii) together with (4.i) and (5) imply that $\varepsilon_j^0 = 0$ for $0 \le j \le J$ and, *a fortiori*, $\|\varepsilon^0\|_{l^1} = 0$. Therefore, (15) yields the first part of (7) with $Q = K_5\,K_4$, with $K_5 = \dfrac{e^{2\,(T+1)\,\|\beta\|_{L^\infty\left([0,a_\dagger)\times[0,T]\right)}}}{2\|\beta\|_{L^\infty\left([0,a_\dagger)\times[0,T]\right)}}$. Using the first estimate of (7) in (13) leads to

$$|\varepsilon_0^{n+1}| \le Q\,k^2 \tag{16}$$

with

$$Q = K_3\,\|D^2(\beta u)\|_{L^\infty\left([0,A^*]\times[0,T]\right)} + K_5\,K_4\|\beta\|_{L^\infty\underline{\mathrm{i}}_{gl}([0,a_\dagger)\times[0,T])}.$$

Next consider $j \ge n$. Combining (10) and (11) we see that

$$|\varepsilon_{j+1}^{n+1}| \le \begin{cases} |\varepsilon_{j-n}^0| & \text{if} \quad j-n \ge J^*, \\ |\varepsilon_{j-n}^0| + \dfrac{K_1K_2T}{24}\,k^2 & \text{if} \quad 0 \le j-n < J^*. \end{cases}$$

This means that, for $0 \le n \le j$,

$$|\varepsilon_{j+1}^{n+1}| \le \frac{K_1K_2T}{24}\,k^2. \tag{17}$$

Similarly, assume now $j < n$. Combining (10) and (11) we see that

$$|\varepsilon_{j+1}^{n+1}| \le |\varepsilon_0^{n-j}| + \frac{K_1K_2T}{24}\,k^2.$$

Combining this relation with (16) we obtain, for $0 \leq j < n$,

$$|\varepsilon_{j+1}^{n+1}| \leq Q\, k^2, \tag{18}$$

with

$$Q = K_3\, \|D^2(\beta u)\|_{L^\infty\left([0,A^*]\times[0,T]\right)} + K_5\, K_4 \|\beta\|_{L^\infty\left([0,a_\dagger)\times[0,T]\right)} + \frac{K_1 K_2 T}{24}.$$

Putting (16), (17) and (18) together yields the second estimate in (7). ∎

Remark: Since singularities in the solution —discontinuities of the function or its derivative— are propagated along characteristics, it is possible to implement numerical methods taking this into consideration and thus maintaining the theoretical order of convergence in spite of the lack of regularity stated in the corresponding convergence theorems [2]. Such discontinuities may arise from lack of smoothness in the initial data or the vital functions, as well as from lack of compatibility between them.

5 Numerical simulations

The first issue we address through numerical simulation is that of whether a maximal age can be identified from the mortality data available in the United States. We shall focus on the female population and use mortality data that is readily available from the Vital Statistics abstracts of the United States.

In view of numerical considerations described and analyzed by Iannelli and Milner in [4], we shall use for the mortality function at advanced ages the specific form $\mu(a) = \frac{C}{(a_\dagger - a)^\alpha}$. The least squares interpolation of mortality data for ages between 80 and 100 using different numbers of data points from both 1990 and 2000 results in the value $a_\dagger = 117$. We therefore assume that the most likely maximal age consistent with the present mortality rates of females in the United States is 117 years.

Next, we present the results of several numerical simulations that bring to light some of the strengths and weaknesses of the model. First, we perform a simulation of the evolution of the female population of the USA from 1990 to 2000. For a projection of the full population two-sex models are necessary. A thorough description of such models and is found in [3].

As explained above, we use the 1-year cohorts reported in the life tables for 1990 and 2000 as initial and final age distributions, respectively, and we use the birth rates and death rates described in Section 3. We show the results of a 10-year simulation using constant-in-time vital rates (autonomous system) and the resulting errors in each age cohort when compared with the final distribution (census 2000 data). The simulations are carried out using a discretization step $k = 1/64$, equivalent to approximately 5.7 days. Similar projections for the decade 1970-1980 are found in [5].

The three initial distributions presented as alternatives in Section 3 result in almost indistinguishable projections. It is therefore advisable to use piecewise constant initial distributions since that is the form in which data are universally gathered and presented.

In contrast, the form we choose for the fertility rate is important, as demonstrated by the comparison table below. The dependence of the fertility rate on age and time is indicated as piecewise constant (p-C), constant (C), or piecewise linear (p-L). For example, the second heading in the table below means the fertility rate is piecewise constant in age and constant in time, i.e. the function in Figure 6.

age cohort \ $\beta(a,t)$	p-C,C	p-L,C	p-C,p-C	p-L,p-L	p-C,p-L
0	3.2%	2.8%	5.5%	-2.8%	4.3%
1	3.2%	2.9%	5.8%	-1.5%	5.6%
2	1.6%	1.1%	5.5%	-2.6%	4.9%
3	1.8%	1.3%	5.6%	-2.0%	5.6%
4	2.8%	2.3%	6.6%	-1.1%	6.6%
5	2.4%	1.9%	5.3%	-1.9%	5.8%
6	2.3%	2.0%	4.6%	-2.7%	4.9%
7	3.2%	3.0%	4.4%	-2.5%	5.0%
8	3.4%	3.3%	4.2%	-2.8%	4.4%
9	4.3%	4.0%	4.3%	-2.1%	4.7%

Table 2: Relative Error in Young Cohort Sizes for Different Forms of Fertility Rate

Comparing the second and third columns as well as the fifth and sixth columns, we can readily see that taking the fertility rate piecewise linear in age leads to smaller errors than taking it piecewise constant in age, whether there is no time dependence or such dependence is expressed as piecewise linear. The case of fertility rates that are piecewise constant in age and in time (fourth column) leads to the worst predictions, with relative errors that may be more than twice as large as those for other choices.

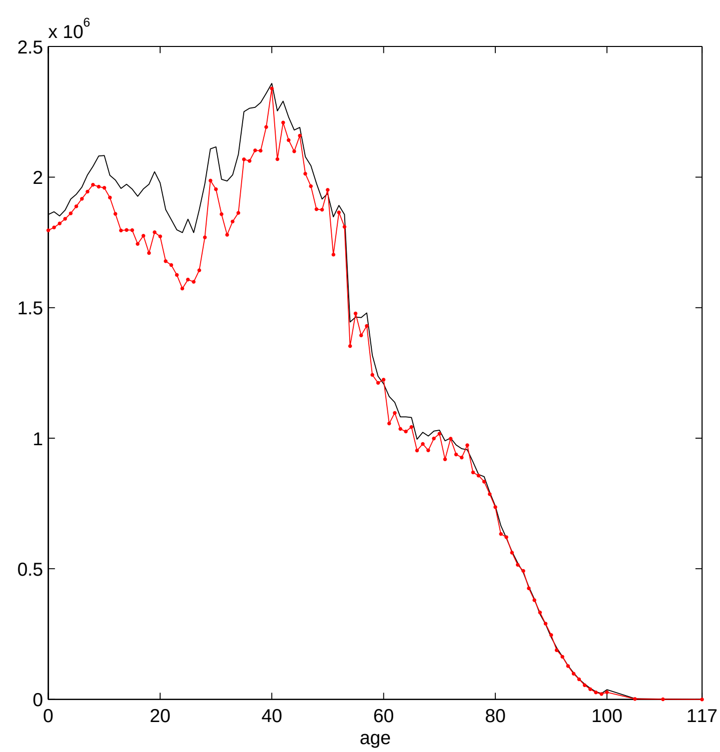

Figure 10: Measured and projected female age density, United States, 2000

We show in Figure 10 the graph of the 2000 census data (in black) together with the final distribution (red dots representing the simulated values using piecewise constant initial data and piecewise linear fertility rate).

We see that there is very good agreement between the two for ages 50 and over, but a noticeable underestimation for ages between 0 and 40, with differences of up to 13% (for 18 year-olds). When we group the data in 5-year cohorts, as most of the population reports do, the differences are somewhat smaller, with a maximal relative error just above 10% for 15-30 year-olds. We show below a bar graph of the data grouped this way.

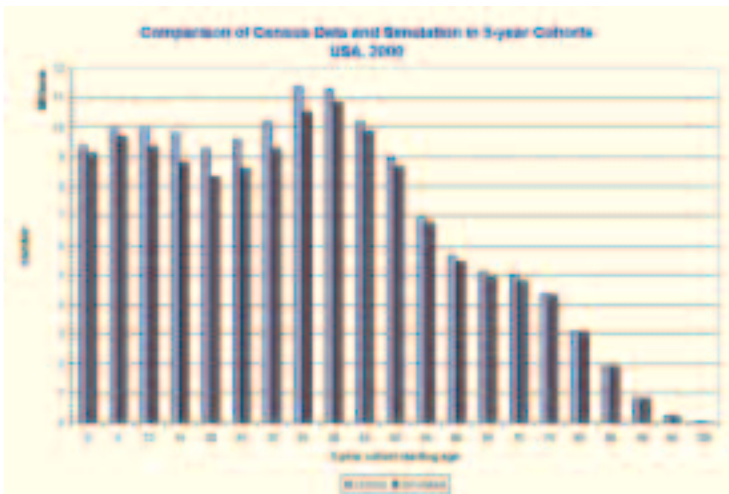

Figure 11: Measured and projected 5-year female cohorts, United States, 2000

Next is a graph of the relative error of the simulated data for the year 2000 with respect to the 2000 census data for 5-year cohorts.

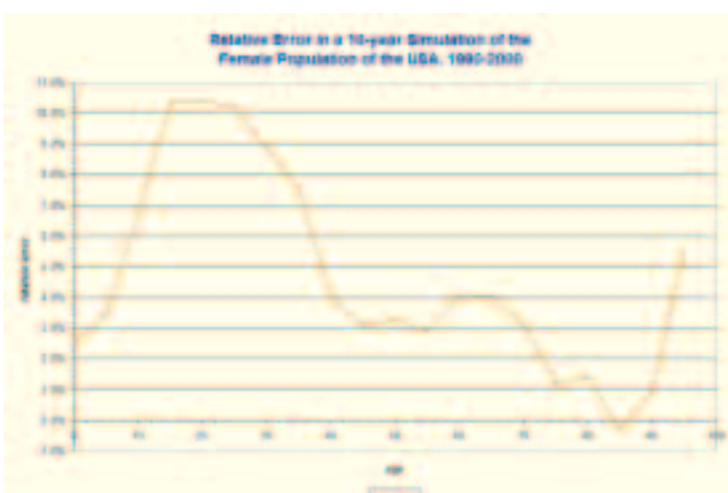

Figure 12: Relative error in projected female age density, United States, 2000

We see that the error for ages 40 to 75 is between 3% and 4%, while that for ages between 75 and 95 is below 1.5%. This is the order of the error that is typical of simulations such as this one when there is no significant migration. The error for the 10 to 40 year old cohorts is between 7% and 10%, and it amounts to 5.4 million women. The majority of this error is due to immigration. The error for the 0 to 10 year-olds is 3%, while that for the 95 to 100 year-olds is 5.4% and that for the oldest cohort—over 100 years of age— is 30%. The large error in this last group is due to its small size combined with the decreasing mortality for the cohort in the intervening decade, which is completely ignored in this simulation since the vital rates are frozen in time at the 1990 levels.

It is straightforward to see what impact a change in the mortality rate $\bar{\mu}_a$ of a given cohort to $\hat{\mu}_a$ has on the predicted value of the size of that cohort ten years later. Using the fact that mortality rates are usually found as piecewise constant over age intervals of five years, we compute the relative error in the predicted size of a cohort of age a in the year 2000 ($t = 10$) using the mortality rates for 1990 ($t = 0$), $\bar{\mu}_a^{(1)}$ of the cohort of age $a - 10$ for the years 1990 to 1995, and $\bar{\mu}_a^{(2)}$ of the cohort of age $a - 5$ for the years 1995 to 2000, as well as the exact mortality rates for the intervening decade, $\mu_a^{(1)}$ of the cohort of age $a - 10$ for the years 1990 to 1995, and $\mu_a^{(2)}$ of the cohort of age $a - 5$ for the years 1995 to 2000.

This leads from the exact relation

$$u(a, 10) = u(a - 10, 0)\, \exp\left(-\int_0^{10} \mu_a\, ds\right) = u(a - 10, 0)\, e^{-5\left(\mu_a^{(1)} + \mu_a^{(2)}\right)},$$

to the erroneous estimate

$$\bar{u}(a, 10) = u(a - 10, 0)\, \exp\left(-\int_0^{10} \bar{\mu}_a\, ds\right) = u(a - 10, 0)\, e^{-5\left(\bar{\mu}_a^{(1)} + \bar{\mu}_a^{(2)}\right)}$$

with a relative error

$$\frac{u(a, 10) - \bar{u}(a, 10)}{u(a, 10)} = 1 - e^{5\left(\left(\mu_a^{(1)} - \bar{\mu}_a^{(1)}\right) + \left(\mu_a^{(2)} - \bar{\mu}_a^{(2)}\right)\right)}.$$

For cohorts aged 15 and above in the year 2000, this is the correct estimate for the potential impact of the changes in mortality rates. For the cohort of individuals aged 10 to 14 in 2000, we should rather use three mortality rates (corresponding to ages 0, 1-4, and 5-9), leading to the following estimate for the relative error in the size of this cohort:

$$\frac{u(10, 10) - \bar{u}(10, 10)}{u(10, 10)} = 1 - e^{\left(\mu_{10}^{(0)} - \bar{\mu}_{10}^{(0)}\right) + 4\left(\mu_{10}^{(1)} - \bar{\mu}_{10}^{(1)}\right) + 5\left(\mu_a^{(2)} - \bar{\mu}_a^{(2)}\right)}$$

where we have used the 1990 mortality rates $\bar{\mu}_{10}^{(0)}$ for the cohort of age 0 in 1990, $\bar{\mu}_{10}^{(1)}$ for the cohort of age 1 from 1991 to 1995, and $\bar{\mu}_{10}^{(2)}$ for the cohort of age 5 from 1995 to 2000, as well as the exact mortality rates for the intervening decade, $\mu_{10}^{(0)}$ for the cohort of age 0 in 1990, $\mu_{10}^{(1)}$ for the cohort of age 1 from 1991 to 1995, and $\mu_{10}^{(2)}$ for the cohort of age 5 from 1995 to 2000.

We show in Table 3 below the potential impact of the change in mortality rate for the simulation from 1990 to 2000. The ages of the cohorts indicated on the table are for the year 2000, and the mortality rates are those for the cohort ten years younger. The actual errors committed are not as large since the changes in mortality rates occurred gradually along the ten- year period, not instantaneously at the beginning of this period.

age cohort \ μ	2000	1990	change	impact
10-14	0.000465	0.0004188	-11.0%	0.0%
15-19	0.000167	0.000192	13.0%	-0.1%
20-24	0.000121	0.0001962	38.3%	-0.1%
25-29	0.000312	0.0004397	29.0%	-0.1%
30-34	0.000460	0.0005525	16.7%	-0.1%
35-39	0.000520	0.0006356	18.2%	-0.2%
40-44	0.000650	0.0008527	23.8%	-0.2%
45-49	0.000967	0.0011571	16.4%	-0.2%
50-54	0.001467	0.0016786	12.6%	-0.4%
55-59	0.002149	0.0026994	20.4%	-0.8%
60-64	0.003253	0.0043683	25.5%	-1.5%
65-69	0.005031	0.006876	26.8%	-2.2%
70-74	0.008087	0.0106811	24.3%	-3.0%
75-79	0.012667	0.0160309	21.0%	-4.5%
80-84	0.019605	0.0250243	21.7%	-7.0%
85-89	0.031018	0.0390903	20.7%	-12.1%
90-94	0.050468	0.0652865	22.7%	-21.0%
95-99	0.087179	0.1104667	21.1%	-41.5%
100-104	0.139619	0.1858182	24.9%	-87.8%

Table 3: Relative Error in Cohort Sizes due to Change in Mortality Rates

The model assumes the population is closed to migration, which is clearly untrue of the population in the united States. We shall see that, actually, the model is very useful in determining an approximation to the age density of immigrants as well as their number. Aside from migration, it is clear that mortality alone is responsible for changes in the size of cohorts of individuals who were 10 years and older in 2000, while fertility is mainly responsible for errors in the size of cohorts of individuals who were under 10 years of age in 2000.

We now show a plot of the difference between the census 2000 1-year cohorts of age 10 to 40 and the simulated data. This should be a very good approximation of the age density of female immigrants to the USA during the 1990's.

Figure 13: Estimated female immigration, United States, 1990-2000

Considering that Table 3 shows a background error—due to uncertainty in the mortality rate—of approximately 0.2% (i.e. 0.12 million from 60,272,111 million aged 10 to 40), we are left with an estimated immigration of approximately 5.3 million women in that age cohort. The available data for that decade shows a total of approximately 8.7 million people legally migrating into the USA, with more men than women typically immigrating. This makes our estimate of the number and age profile of women immigrants in the cohort of 10-to-40-year-olds quite credible and, probably, quite accurate. Is it likely that some 4 million women aged 10 to 40 immigrated legally into the USA during the decade from 1990 to 2000 (45% of all immigrants), and approximately 1.3 million illegally.

It is worth pointing out that, since very few individuals immigrate at ages between 75 and 95, it is safe to assume that the dynamics of those cohorts is quite accurately described by the model and the small errors we see are due to variations in the mortality rates.

For our final simulation, from the year 2000 to 2010, we need to make projections for the changes in mortality and fertility rates. We do this by using mortality and fertility data from 1970, 1980, 1990, and 2000, and finding the best least squares fit of the data by an exponential or (regression) line. Since the data for fertility is non-zero only for the cohorts of ages 10- 14, 15-17, 18-19, 20-24, 25-29, 30-34, 35-40, 40-45, and 45-49, we find nine curves of best fit, one for each age cohort. The fertility function we use for our simulation is constant in age within each cohort and varying in time according to the exponential or line of best fit for each of the age cohorts. We present below a graph of the fertility rate thus defined. Along the x-axis we have age from 0 to 60 years in reverse order, along the y-axis we have the time variable (calendar year) from 2000 to 2010, and along the z-axis we have the corresponding fertility rate $\beta(a,t)$.

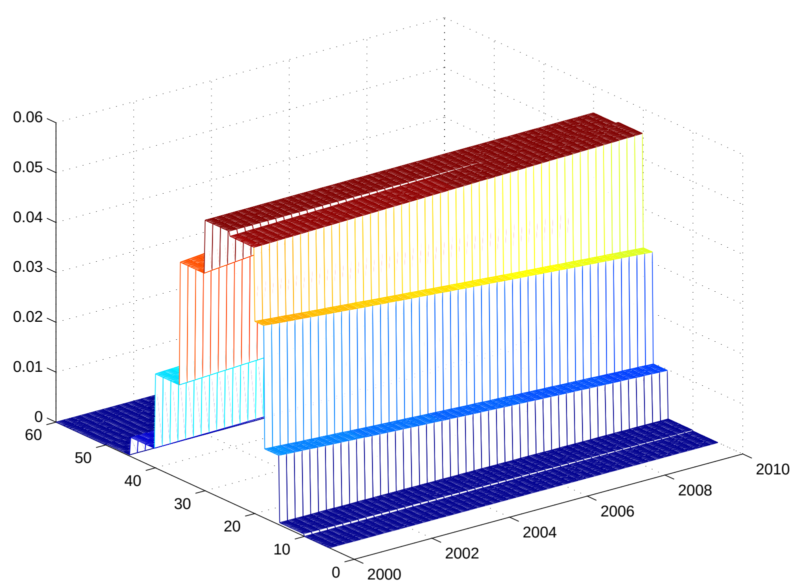

Figure 14: Extrapolated fertility rate, United States, 2000-2010

Similarly, since the mortality data is usually found for age cohorts 0, 1-4, 5- 9, 10-14, . . ., 80-84, 85 and above, we find seventeen exponential curves of best fit, one for each age cohort up to 80 years of age. The mortality function we use for our simulation is piecewise linear in age for ages from 0 to 80, constructed analogously to that for the simulation from 1990 to 2000, and varying in time according to the exponential best fit for each of the age cohorts. For ages over 80 years we use the mortality rate defined for the year 2000, as explained above. We present below a graph of the mortality rate thus defined. Along the x-axis we have the age variable from 0 to 80 years in reverse order, along the y-axis we have the time variable (calendar year) from 2000 to 2010, and along the z-axis we have the corresponding mortality rate $\mu(a, t)$.

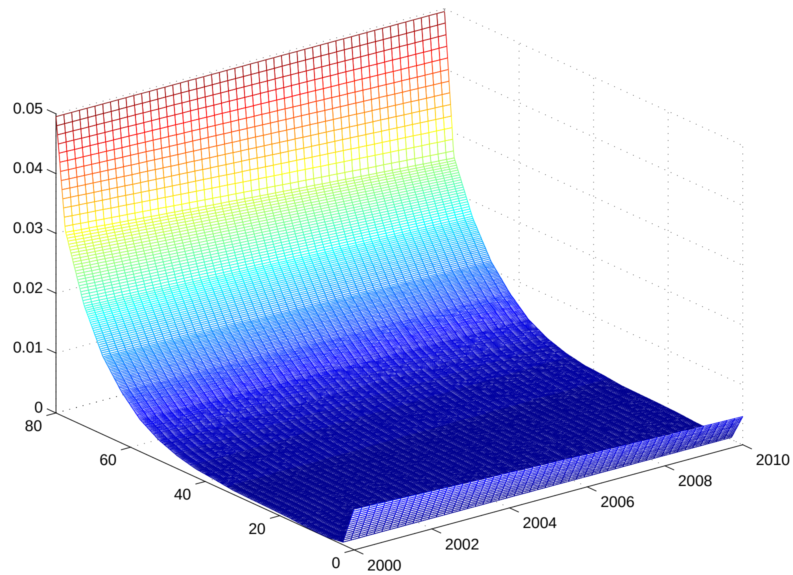

Figure 15: Extrapolated mortality rate, United States, 2000-2010

We present next the graph of the projected age density of females in the USA in the year 2010, together with the year 2000 distribution as given by census data.

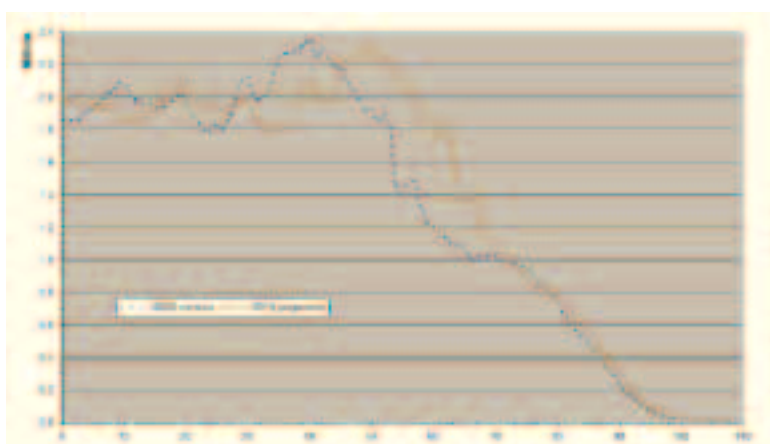

Figure 16: Graph of the female age density, United States, 2000 and 2010

Finally, we include a histogram of the projected 5-year female age cohorts for 2010.

Figure 17: female 5-year age cohorts, United States, 2010

6 Conclusions

First we found through data fitting the female mortality rates in the United States for 1990 and 2000 that the likely maximal age for this population is 117 years. It is quite likely that such age might increase, albeit very slowly, since mortality rates in all age cohorts for both genders have a tendency to decline slowly over time.

The simulations performed for the evolution of the female population of the United States from 1990 to 2000 underscore several important issues in projecting population growth. First, the regularity of the initial conditions makes little difference to the accuracy of the projections. The major sources of error for projecting the size of cohorts over 10 years of age are immigration in the first place, and a decrease in the mortality rate in the second place. As we show in Table 3, for cohorts over 50 years of age in 1990 the mortality rates changed between 21% and 27% during the following decade, leading to a potential error between 1% and 55% in the projected size of the corresponding cohorts 10 years later.

For the younger ages—from 0 to 10 years—changing fertility rates could potentially result in large errors in projected values. In the decade from 1990 to 2000 the fertility rate for women from 35 to 40 years of age increased by 42%, while that for women between 40 and 45 years of age nearly doubled. In spite of such large changes, in this particular decade the errors in projecting young cohorts were not too large because the increases in fertility rates just mentioned were accompanied by decreases in the 10%-20% range for teenage and young adult women.

We see as we compare results from many different simulations that in making 10- year projections for the population of the USA there are essentially 5 major age cohorts in terms of model predictive capability. The very young (0 to 10 years of age) are the only cohort prone to errors due to variations in fertility rates. The young (10 to 40 years of age) are the ones suffering from the largest absolute errors because of immigration, with relative errors approximately 10%. The mature ages (40 to 75 years) have relative errors half that size because of a combination of some immigration and the larger impact of variations in mortality rates. The old ages (75 to 95 years) are the easiest to project since there is hardly any immigration and mortality rates are quite stable. Finally, the very advanced ages (over 95 years) show large relative errors because of their small size and the relatively large variablity in mortality rates.

Concerning the simulation made to project the female population of the United States in 2010, we can expect errors of approximately 10% for cohorts below 40 years of age, and approximately half that much for cohorts between 40 and 75 years of age. For cohorts between 75 and 95 we should expect errors in the range of approximately 1% to 2%.

Acknowledgements: O. Angulo and J.C. López-Marcos were supported in part by the project of the Ministerio de Ciencia y Tecnología BFM2002-01250 and by the project of the Junta de Castilla y León and Unión Europea F.S.E. VA063/04. F. A. Milner was supported in part by the National Science Foundation under Grant DMS-0314575.

References

[1] L. M. Abia, O. Angulo and J. C. López-Marcos, Age-structured population dynamics models and their numerical solutions, *Ecol. Modelling*, **188** (2005), 112-136.

[2] O. Angulo, J. C. López-Marcos and M. A. López-Marcos, A numerical integrator for a model with a discontinuous sink term: the dynamics of the sexual phase of monogonont rotifera, *Nonlinear Anal. R.W.A.* **6** (2005), 935-954.

[3] Iannelli, M., Martcheva, M. and Milner, F. A., Gender-Structured Population Modeling: Mathematical Methods, Numerics and Simulations, SIAM: Philadelphia, April 2005.

[4] Iannelli, M. and Milner, F. A., On the approximation of the Lotka-McKendrick equation with finite life-span, *J. Comp. Appl. Math.* **136**: 245-254 (2001).

[5] Milner, F. A. and Rabbiolo, G., Rapidly Converging Numerical Algorithms for Models of Population Dynamics, *J. Math. Biol.* **30**: 733-753 (1992).

[6] *Vital Statistics of the United States* **Vol. II**, Section 6: Table 6-2 (September 1994). 1990 Life Tables: Number of Survivors at Single Years of Age.

[7] *National Vital Statistics Reports* **51**, No. 3: Table 3 (December 19, 2002). Life table for females: United States, 2000.